E2-2020-24

I. Zborovský [1,*], M. V. Tokarev [**]

SELF-SIMILARITY, FRACTALITY AND ENTROPY PRINCIPLE IN COLLISIONS OF HADRONS AND NUCLEI AT TEVATRON, **RHIC** AND **LHC**

---

[1] Nuclear Physics Institute of the Czech Academy of Sciences, Řež, Czech Republic
* E-mail: zborovsky@ujf.cas.cz
** E-mail: tokarev@jinr.ru

Зборовский И., Токарев М. В.   E2-2020-24

Самоподобие, фрактальность и принцип энтропии в столкновениях адронов и ядер на Tevatron, RHIC и LHC

Обосновывается z-скейлинг инклюзивных спектров как проявление самоподобия и фрактальности адронных взаимодействий. Установлено скейлинговое поведение рождения отрицательно заряженных адронов в Au + Au-столкновениях на RHIC в рамках программы BES-I. Скейлинговая функция $\psi(z)$ как функция переменной подобия z зависит от модельных параметров — фрактальных размерностей и «удельной теплоемкости», а ее форма не зависит от энергии и центральности столкновения и типа инклюзивной частицы. В рамках теории z-скейлинга, учитывающего принцип максимума энтропии, оценена зависимость величины энергетических потерь конституентов от энергии и центральности столкновения и импульса регистрируемой частицы. Сформулирован новый закон сохранения, учитывающий фрактальные размерности и доли импульсов конституентов. Обсуждается возможность квантования фрактальных размерностей.

Zborovský I., Tokarev M. V.   E2-2020-24

Self-Similarity, Fractality and Entropy Principle in Collisions of Hadrons and Nuclei at Tevatron, RHIC and LHC

The z-scaling of inclusive spectra as a manifestation of self-similarity and fractality of hadron interactions is illustrated. The scaling for negative particle production in Au + Au collisions from BES-I program at RHIC is demonstrated. The scaling function $\psi(z)$ as a function of self-similar variable z depends on the model parameters — the fractal dimensions and "specific heat", and reveals energy, multiplicity, and flavor independence. Based on the maximum entropy principle and z-scaling, energy loss as a function of the collision energy, centrality, and transverse momentum of inclusive particle is estimated. New conservation law including fractal dimensions and momentum fractions is found. Quantization of fractal dimensions is discussed.

INTRODUCTION

The production of particles with high transverse momenta from the collisions of hadrons and nuclei at sufficiently high energies has relevance to constituent interactions at small scales. In this regime, it is interesting to search for new physical phenomena in elementary processes, such as quark compositeness [1, 2], extra dimensions [3–7], black holes [8–10], fractal space-time [11–13], fundamental symmetries [14], etc. Other aspects of high energy interactions are connected with small momenta of secondary particles and high multiplicities. In this regime, collective phenomena of particle production take place. Search for new physics in both regions is one of the main goals of investigations at the Relativistic Heavy Ion Collider (RHIC) at BNL and the Large Hadron Collider (LHC) at CERN. Processes with high transverse momenta of produced particles are most suitable for a precise test of perturbative Quantum Chromodynamics (QCD). The soft regime is preferred for verification of nonperturbative QCD and investigation of phase transitions in non-Abelian theories. Basic principles which lie in the root of modern physical theories are the principles of relativity (special, general, scale), gauge invariance, locality, spontaneous symmetry breaking and others. The fundamental property of asymptotic freedom and gauge invariance were used for the development of QCD, the theory of strong interactions of quarks and gluons. Due to asymptotic freedom, the perturbative QCD is controlled by higher-order corrections in strong coupling constant. However, there is no universal method to be used in the nonperturbative sector of QCD. This is a big challenge because even at large momentum transfer, some nonperturbative aspects of the theory are still needed to make a comparison with measured physical observables. Moreover, the internal structure of hadrons is not fully understood and remains largely mysterious especially at small scales. In such a situation, the principles of self-similarity and fractality can give additional constrains for theories in particle physics. We consider that both mentioned principles reflect general features of hadron interactions at high energies. They are important for verification of symmetries already established, study of their possible violations, and search for new symmetries which govern physical theories.

1. SCALING AND UNIVERSALITY AS GENERAL CONCEPTS

The idea of self-similarity of hadron interactions is a fruitful concept to study collective phenomena in hadron matter. Important manifestation of such a concept is existence of scaling itself (see [15–17] and references

1

therein). Scaling in general means self-similarity at different scales. The physical content meant behind it can be of different origin. Some of the scaling features constitute pillars of modern critical phenomena. Other category of scaling laws (self-similarity in point explosion, laminar and turbulent fluid flow, super-fluidity far from phase boundary and critical point, etc.) reflects features not related to phase transitions.

The notions "scaling" and "universality" have special importance in critical phenomena. The scaling means that the system near the critical point exhibiting self-similar properties is invariant under transformation of a scale. According to universality, quite different systems behave in a remarkably similar way near the respective critical point. The universality hypothesis reduces the great variety of critical phenomena to a small number of equivalence classes, the so-called "universality classes", which depend only on a few fundamental parameters (critical exponents). The universality has its origin in the long-range character of interactions (fluctuations and correlations). Close to the transition point, the behavior of the cooperative phenomena becomes independent of the microscopic details of the considered system. The fundamental parameters determining the universality class are the symmetry of the order parameter and the dimensionality of space.

2. z-SCALING

The z-scaling belongs to the scaling laws with applications not limited to the regions near a phase transition. The scaling regularity concerns hadron production in the high energy proton (antiproton) and nucleus collisions (see [18–22] and references therein). It manifests itself in the fact that the inclusive spectra of various types of particles are described with a universal scaling function $\psi(z)$. The function $\psi(z)$ depends on a single variable z in a wide range of the transverse momentum, registration angle, collision energy, and centrality. The scaling variable has the form

$$z = z_0 \, \Omega^{-1}. \tag{1}$$

The quantity $z_0 = \sqrt{s_\perp} / [(dN_{\mathrm{ch}}/d\eta|_0)^c m_N]$ is proportional to the transverse kinetic energy $\sqrt{s_\perp}$ of a selected binary subprocess responsible for production of the inclusive particle with mass m_a and its partner (antiparticle) with mass m_b. The multiplicity density $dN_{\mathrm{ch}}/d\eta|_0$ of charged particles in the central interaction region, the nucleon mass m_N, and the parameter c, interpreted as a "specific heat" of the produced medium, completely determine the value of z_0. The quantity Ω is the maximal relative number of configurations containing binary subprocesses defined by the momentum fractions x_1 and x_2 of colliding hadrons (nuclei), which carry interacting constituents, and by the momentum fractions y_a and y_b of objects created directly in these subprocesses, which carry the inclusive particle and its antiparticle counterpart, respectively. The relative number of the configurations is given by the function

$$\Omega = (1 - x_1)^{\delta_1}(1 - x_2)^{\delta_2}(1 - y_a)^{\varepsilon_a}(1 - y_b)^{\varepsilon_b}, \tag{2}$$

2

where δ_1 and δ_2 are fractal dimensions of the colliding objects, and ε_a and ε_b are fractal dimensions of the fragmentation process in the scattered and recoil directions, respectively. The selected binary interaction of the constituents used for calculation of the transverse kinetic energy $\sqrt{s_\perp}$ and z_0, is defined by the maximum of $\Omega(x_1, x_2, y_a, y_b)$ with the kinematic constraint

$$\left(x_1 P_1 + x_2 P_2 - \frac{p}{y_a}\right)^2 = M_X^2. \tag{3}$$

The mass $M_X = x_1 M_1 + x_2 M_2 + m_b/y_b$ of the recoil system in the subprocess is expressed via momentum fractions and depends implicitly on 4-momenta of the colliding objects and the inclusive particle, P_1, P_2 and p, respectively. Constraint (3) accounts for the locality of hadron interaction at the constituent level and sets a restriction on the momentum fractions via kinematics of the constituent subprocess. The function Ω^{-1} represents a resolution at which a subprocess defined by the fractions x_1, x_2, y_a, y_b can be singled out of the inclusive reaction. The scaling variable z has property of a fractal measure. It grows in a power-like manner with the increasing resolution Ω^{-1}.

The scaling function $\psi(z)$ is expressed in terms of the experimentally measured inclusive invariant cross section $Ed^3\sigma/dp^3$, the multiplicity density $dN/d\eta$, and the total inelastic cross section σ_{in} as follows [20]:

$$\psi(z) = \frac{\pi}{(dN/d\eta)\ \sigma_{\text{in}}} J^{-1} E \frac{d^3\sigma}{dp^3}. \tag{4}$$

Here J is the Jacobian for the transformation from $\{p_T^2, y\}$ to $\{z, \eta\}$. The Jacobian depends on kinematic variables characterizing the inclusive reaction. The multiplicity density in expression (4) concerns particular hadron species. The function $\psi(z)$ is normalized to unity

$$\int\limits_0^\infty \psi(z)\, dz = 1 \tag{5}$$

and interpreted as a probability density to produce an inclusive particle with the corresponding value of the self-similarity variable z. The flavor independence of z-presentation of inclusive spectra means that the shape of the scaling function $\psi(z)$ is the same for hadrons with different flavor content over a wide range of z [19, 20]. The scale transformation

$$z \to \alpha_F z, \quad \psi \to \alpha_F^{-1}\psi \tag{6}$$

is used for the comparison of the shapes of the scaling function for different hadron species. The scale parameter α_F depends on type (F) of the produced particles. The transformation preserves normalization (5) and does not destroy the energy, angular, and multiplicity independence of the z-presentation of particle spectra.

2.1. Identified Hadrons in $p + p$ Collisions at RHIC. Let us remind the properties of z-presentation of experimental data already found in proton–(anti)proton collisions at high energies. These are the energy, angular, and multiplicity independence of scaling function $\psi(z)$ for different types of hadrons, direct photons, and jets confirmed by numerous data obtained at U70, ISR, Sp$\bar{\text{p}}$S, Tevatron, and RHIC. The energy independence of the z-presentation of inclusive spectra means that the shape of the scaling function is independent of the collision energy $\sqrt{s}$ over a wide range of the transverse momentum p_T of produced inclusive particle. Some results on the energy independence of the z-scaling for hadron production in proton–proton collisions were presented in [19]. The analyzed data include negative pions, kaons, and antiprotons measured at the FNAL, ISR, and RHIC energies. The spectra were measured over a wide transverse momentum range $p_T = 0.1–10$ GeV/c. The cross sections decrease from 10^2 to 10^{-10} mb/GeV^2 in this range. The strong dependence of the spectra on the collision energy $\sqrt{s}$ increases with transverse momentum.

Figure 1, a shows the z-presentation of the spectra of $\pi^-, K^-, \overline{p}$, and Λ particles produced in $p + p$ collisions over the range $\sqrt{s} = 19–200$ GeV and $\theta_{\text{cms}} = 3–90°$. The symbols correspond to the data on differential cross sections measured in the central [24–33] and fragmentation [23] regions, respectively. The analysis comprises the inclusive spectra of particles [26, 27] measured up to very small transverse momenta ($p_T \simeq 45$ MeV/c for pions and $p_T \simeq 120$ MeV/c for kaons or antiprotons). One can see that the distributions of different hadrons are sufficiently well described by a single curve over a wide range of $z = 0.01–30$. The scaling function $\psi(z)$ changes more than ten orders of magnitude. The solid lines represent the same curve
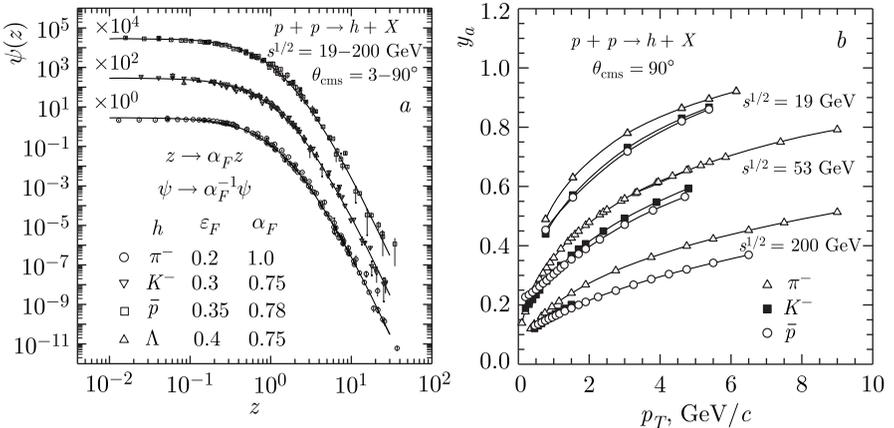

Fig. 1. a) The inclusive spectra of π^-, K^-, $\overline{p}$, and Λ hadrons produced in $p + p$ collisions in z-presentation. Data are taken from [23–33]. b) The dependence of the fraction y_a on the transverse momentum p_T for π^-, K^-, and $\overline{p}$ produced in $p + p$ collisions at $\sqrt{s} = 19, 53$, and 200 GeV in the central rapidity region

shifted by multiplicative factors for reasons of clarity. The same holds for the corresponding data shown with the different symbols.

The z-presentation of the transverse momentum distributions in proton–proton collisions was obtained for $\delta_1 = \delta_2 \equiv \delta$. We assume that the main features of the fragmentation processes in the scattered and recoil directions can be described by the same parameter $\varepsilon_a = \varepsilon_b \equiv \varepsilon_F$ which depends on type (F) of the inclusive particle. The independence of the scaling function $\psi(z)$ from multiplicity and energy was found for the constant values of the parameters $c = 0.25$ and $\delta = 0.5$. The angular independence of $\psi(z)$ at small angles is sensitive to the values of $m_b = m(\pi^+)$, $m_b = m(K^+)$, and $m_b = m(p)$, for the inclusive production of π^-, K^-, and antiprotons, respectively. The parameter ε_F $(\varepsilon_\pi = 0.2, \varepsilon_K \simeq 0.3, \varepsilon_{\overline{p}} \simeq 0.35, \varepsilon_\Lambda \simeq 0.4)$ increases with the mass of the produced hadron. The indicated values of the parameters are consistent with the energy, angular, and multiplicity independence of the z-presentation of spectra for all types of the analyzed inclusive particles $(\pi, K, \overline{p}, \Lambda)$. The parameters were found to be independent of kinematic variables $(\sqrt{s}, p_T,$ and $\theta_{\mathrm{cms}})$. The scale factors α_F are constants which allow us to describe the z-presentation of inclusive spectra for different hadron species by a single curve. Based on the obtained results [19], we conclude that the RHIC data on $p + p$ collisions confirm the flavor independence of the z-scaling including production of particles with very small p_T.

The method of construction of the scaling variable z fixes values of the corresponding momentum fractions. The dependence of the fractions y_a and y_b on the kinematic variables $(p_T, \theta_{\mathrm{cms}}, \sqrt{s})$ describes features of the fragmentation processes. The fraction y_a characterizes dissipation of the energy and momentum of the object produced by the underlying constituent interaction into the near side of the inclusive particle. This effectively includes energy loss of the scattered secondary partons moving in the direction of the registered particle as well as feed down processes from prompt resonances out of which the inclusive particle may be created.

Figure 1, b shows the dependence of the fraction y_a on the transverse momentum p_T of $\pi^-, K^-, \overline{p}$ particles produced in $p + p$ collisions at the energies $\sqrt{s} = 19, 53, 200$ GeV and $\theta_{\mathrm{cms}} = 90°$. All curves demonstrate a nonlinear monotonic growth with p_T. It means that the relative energy dissipation associated with the production of a high-p_T particle is smaller than for the inclusive processes with lower transverse momenta. This feature is similar for all inclusive reactions at all energies. The decrease of the fractions y_a with the increasing collision energy is another property of the considered mechanism. It corresponds to more energy dissipation at higher energies. This can be due to the larger energy losses and/or due to the heavy prompt resonances. The third characteristic is a slight decrease of y_a with the mass of the inclusive particle. It implies more energy dissipation for creation of heavier hadrons compared to hadrons with smaller masses.

2.2. Strangeness Production in $p + p$ Collisions at RHIC. The strange particles represent a special interest as they contain strange quarks which are the lightest quarks absent in the net amount in the initial state. At the same time, the strange quarks created in the constituent subprocesses are substantially heavier than the valence quarks in the colliding protons. The self-similarity of such interactions, expressed by the same form of the scaling function, results in different properties of the constituent collisions and fragmentation processes as compared to those which underlay the production of the nonstrange particles. The scaling behavior of $\psi(z)$ for strange particles could give more evidence in support of unique description of $p + p$ interaction at a constituent level and could provide a good basis for study of peculiarities of the strangeness production in nuclear collisions, as well as for study of the origin of the strangeness itself.

The self-similarity of strange hadron production was studied [20] using data [36–39] on inclusive cross sections of K_S^0, K^-, K^{*0}, ϕ mesons measured in proton collisions at RHIC. The data on strange particle spectra [24, 41–48] obtained by the BS, CCRS, CDHW, AFS, NA61/SHINE, and NA49 collaborations were used in the analysis as well.

Figure 2, a shows z-presentation of the transverse momentum spectra [33–39] of strange mesons and baryons measured in $p + p$ collisions at the energy $\sqrt{s} = 200$ GeV in the central rapidity region at RHIC. The symbols representing data on differential inclusive cross sections include baryons which consist of one, two, and three strange valence quarks. The multiplicative factors $10^0, 10^{-1}$, and 10^{-2} are used to show the data z-presentation separately for mesons, single-strange ($\Lambda, \Lambda^*, \Sigma^*$) and multi-strange ($\Xi^-, \Omega$) baryons, respectively. The symbols for different particles are shown for the
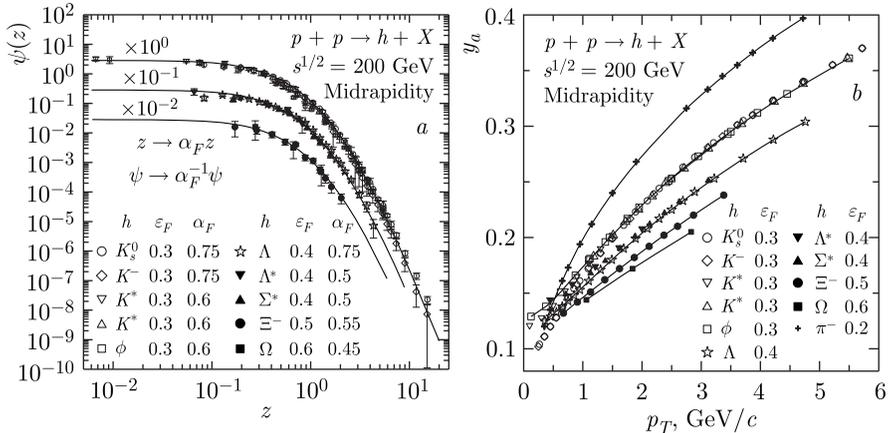

Fig. 2. Scaling function $\psi(z)$ (a) and momentum fraction y_a (b) for strange (K_S^0, K^-, $K^{*0}, \phi, \Lambda, \Lambda^*, \Sigma^*, \Xi^-, \Omega$) hadrons produced in $p + p$ collisions at $\sqrt{s} = 200$ GeV and $\theta_{\mathrm{cms}} \simeq 90°$. Experimental data are taken from [33–39]. The solid line in (a) corresponds to $\psi(z)$ for π^- mesons [32, 40]. The points in (a) and (b) are calculated for $\delta = 0.5$ and for the indicated values of ε_F and α_F

indicated values of the parameters ε_F and α_F. They are reasonably well described by the solid curve representing a reference line ($\alpha_\pi = 1$) for π^- mesons obtained from analysis [19] of pion spectra. It is consistent with the energy, angular, and multiplicity independence of the scaling function for different hadrons. The fragmentation dimension ε_F for strange mesons is larger than for pions ($\varepsilon_\pi = 0.20 \pm 0.01$). It suggests larger energy loss by production of mesons with strangeness content. The fragmentation dimension for strange baryons grows with the number of the strange valence quarks.

Figure 2,b demonstrates the p_T-dependence of the momentum fraction y_a of strange hadrons and π^- mesons produced in $p + p$ collisions at $\sqrt{s} = 200$ GeV. The fraction y_a increases with the transverse momentum for all particles. The energy loss $\Delta E_q/E_q = (1 - y_a)$ depends on value of the fragmentation dimension ε_F. As one can see, the relative energy loss decreases with the increasing p_T for all particles. For a given $p_T > 1$ GeV/c, the energy loss is larger for strange baryons than for strange mesons. The growth indicates increasing tendency with larger number of strange valence quarks inside the strange baryon, $(\Delta E/E)_\Omega > (\Delta E/E)_{\Xi^-} > (\Delta E/E)_\Lambda \simeq \simeq (\Delta E/E)_{\Lambda^*} \simeq (\Delta E/E)_{\Sigma^*}$.

2.3. Top-Quark Production at LHC and Tevatron. The top quark is the heaviest known elementary particle. It was discovered at the Tevatron in 1995 by the CDF and DØ collaborations [49, 50] at a mass of around 170 GeV. The first measurements of the differential cross section as a function of the transverse momentum of the top quark were presented by the DØ collaboration [51]. It is expected that *top* physics is extremely important in the search for new and for the study of known symmetries in high-p_T region.

Figure 3 shows the z-presentation [22] of the spectra of top-quark production obtained in $p + p$ collisions at the LHC energies $\sqrt{s} = 7, 8$, and 13 TeV in the central rapidity region. The measurements of the inclusive cross sections were performed by the CMS [52–55] and ATLAS [56–59] collaborations in the dilepton and jet channels. The data include measurements over a wide range of the transverse momentum $30 < p_T < 1000$ GeV/c. The z-scaling of π^--meson spectra shown by the solid line serves as a reference curve. The values of the fractal dimension $\delta = 0.5$ and the parameter $c = 0.25$ are the same as used in our previous analyses [19, 20] for other hadrons. We have set $\varepsilon_{\text{top}} = 0$, as negligible energy loss is assumed in the elementary $t\bar{t}$ production process. The scale parameter α_F in transformation (6) is found to be $\alpha_{\text{top}} \simeq 0.0045$. The data on the top-quark production [60] in $\overline{p} + p$ collisions obtained by the DØ collaboration at the Tevatron energy $\sqrt{s} = 1.96$ TeV are compatible with the LHC data in z-presentation. The scaling function $\psi(z)$ demonstrates energy independence over a wide range of the self-similarity parameter z.

Based on the above comparison, we conclude that the LHC and Tevatron data on inclusive spectra of the top quark support the flavor independence of the scaling function $\psi(z)$ over the interval of $z = 0.01-8$. This result gives us indication on the self-similarity of top-quark production in $p + p$ and $\overline{p} + p$
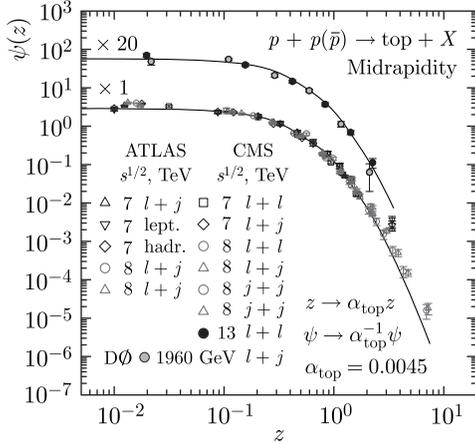
Fig. 3. The scaling function $\psi(z)$ of the top-quark production in $p + p$ and $\overline{p} + p$ collisions at the LHC energies $\sqrt{s} = 7, 8, 13$ TeV and the Tevatron energy $\sqrt{s} = 1.96$ TeV. The symbols denote the experimental data obtained by the CMS [52–55], ATLAS [56–59], and DØ [60] collaborations. The solid line is a reference curve corresponding to π^--meson production in $p+p$ collisions

interactions up to the top-quark transverse momentum $p_T = 1$ TeV/c and for a wide range of the collision energy $\sqrt{s} = 1.96, 7, 8$, and 13 TeV.

2.4. Jet Production at LHC and Tevatron. Jets are traditionally considered as the best probes of constituent interactions at high energies. They are of interest both for study of properties of the jet itself and in search for new particles identified by the jets. In hadron collisions, jet is a direct evidence of hard interaction of hadron constituents (quarks and gluons). The data on inclusive cross sections of jet production in $p + p$ collisions at the LHC energies $\sqrt{s} = 2760, 7000$, and 8000 GeV [61–66] were analyzed [22] in the framework of z-scaling. We used the parameter values $c = 1$, $\delta = 1$, $\varepsilon_{\mathrm{jet}} = 0$, and $m_a = m_b = 0$ for the analysis. The results are compared with z-presentation of jet spectra in $\overline{p} + p$ collisions at the Tevatron energies $\sqrt{s} = 630, 1800, 1960$ GeV [67–78].

Figure 4, a shows p_T-dependence of jet spectra measured in the central pseudorapidity window $|\eta| < 0.5$ by the ATLAS [61–63], CMS [64, 65], and ALICE [66] collaborations at the LHC and the spectra obtained in the midrapidity region by the DØ [67–72] and CDF [73–78] collaborations at the Tevatron. The data collected by the CMS collaboration at $\sqrt{s} = 8000$ GeV correspond to the integrated luminosity of 19.7 fb^{-1}. The spectra were measured up to the transverse momentum $p_T = 2500$ GeV/c. The measurement based on the data collected with the ATLAS detector at $\sqrt{s} = 8000$ GeV corresponds to an integrated luminosity of 20.2 fb^{-1}. The ATLAS data cover the range $70 < p_T < 2500$ GeV/c. The distributions change by many orders of magnitude within the analyzed p_T-range. As can be seen
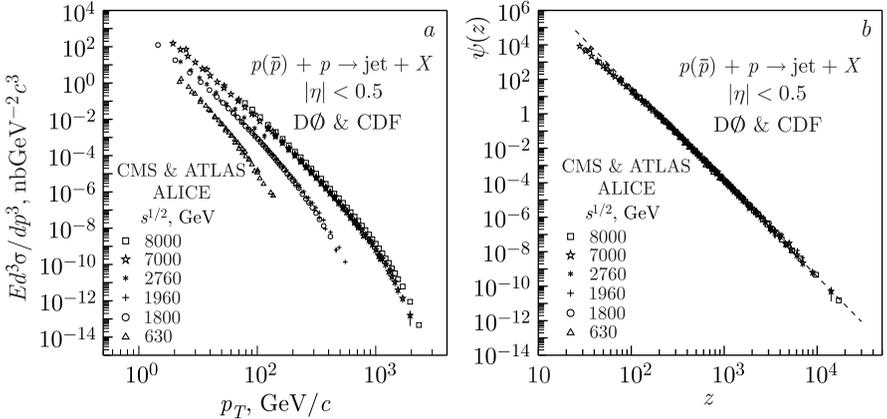
8

Fig. 4. The inclusive spectra of jet production in $p + p$ and $\overline{p} + p$ collisions in p_T- (a) and z-presentation (b) measured at $\theta \simeq 90°$. The symbols denote the ATLAS [61–63], CMS [64, 65], and ALICE [66] data obtained in $p + p$ collisions at $\sqrt{s} = 2760, 7000, 8000$ GeV and the DØ [67–72] and CDF [73–78] data obtained in $\overline{p} + p$ collisions at $\sqrt{s} = 630, 1800, 1960$ GeV

from Fig. 4, a, the strong dependence of the spectra on the collision energy $\sqrt{s}$ increases with the transverse momentum.

Figure 4, b demonstrates the energy independence of $\psi(z)$ for jet production and its power behavior over the range $\sqrt{s} = 630-8000$ GeV at $\eta \simeq 0$. The scaling function changes more than twelve orders of magnitude and can be described by a power law $\psi(z) \sim z^{-\beta}$ over a wide z-range. The slope parameter β is energy independent in the large region of $\sqrt{s}$. The dashed line corresponds to the asymptotic behavior of $\psi(z)$. The data obtained at the LHC confirm results of the analysis [79] of jet spectra measured by the DØ and CDF collaborations in $\overline{p} + p$ collisions at the Tevatron with parameters $\delta = 1$ and $c = 1$.

2.5. BES-I Program in Au + Au Collisions at RHIC. Experimental results from RHIC and LHC support the hypothesis that a new state of nuclear matter is created in the collisions of heavy ions at high energy. The created matter with quark and gluon degrees of freedom, the Quark–Gluon Plasma, reveals features of a strongly-coupled medium. It is assumed that the medium produced in heavy-ion collisions is thermalized. The phase diagram of nuclear matter is usually presented in the temperature-baryon chemical potential plane $\{T, \mu_B\}$. Both quantities can be varied by changing the energy and centrality of the nuclear collisions and the type and momentum of the produced particles. The idea of the Beam Energy Scan (BES) program at RHIC is to scan the phase diagram of nuclear matter from the top RHIC energy to the lowest possible energy achievable on this collider and to compare it with the phase diagram predicted by the QCD theory [80, 81]. The program is aimed to perform systematic investigation and data analysis of particle production in the heavy-ion interactions over a wide range of collision energy and centrality.

9

The systematic measurements performed with heavy ions are of great interest to search for critical phenomena in a broad range of kinematic variables.

We extend the applicability of the self-similarity principle to the description of hadron production in nucleus–nucleus collisions. The self-similarity concerns fractal structure of the colliding objects, interaction of their constituents, and fractal character of fragmentation processes in the final state. This physical principle is assumed to be valid also in the high-density and high-temperature phase in which quark and gluon degrees of freedom dominate.

Figure 5, a shows the scaling function $\psi(z)$ for negative hadrons [21] produced in the $0-5\%$ central Au + Au collisions at different energies $\sqrt{s_{NN}} = 7.7-200$ GeV. The symbols correspond to the spectra [82] measured by the STAR collaboration in the pseudorapidity window $|\eta| < 0.5$. The z-presentation of the spectra demonstrates energy independence of the function $\psi(z)$ over the analyzed kinematic range. Moreover, the symbols representing the nuclear data are in reasonable agreement with the solid curve which depicts the z-scaling of h^- particles produced in $p + p$ collisions over the range $\sqrt{s} = 11.5-200$ GeV. The same energy independence of $\psi(z)$ is valid [21] for different centrality classes of Au + Au collisions.

The scaling was obtained for the multiplicity-dependent fragmentation dimension in the form $\varepsilon_{\mathrm{AuAu}} = \varepsilon_0(2dN_{\mathrm{neg}}^{\mathrm{AuAu}}/d\eta) + \varepsilon_{pp}$ with a suitable choice of ε_0, and for the constant values of the model parameters $c_{\mathrm{AuAu}} = 0.11$, $\delta_A = A\delta$, $\delta = 0.5$, and $\varepsilon_{pp} = 0.2$ at $\sqrt{s_{NN}} \gtrsim 19.6$ GeV. The parameter ε_0 shows logarithmic increase with $\sqrt{s_{NN}}$ [21]. It reflects growing tendency of the suppression of hadron yields in the central collisions of heavy nuclei as the collision energy and multiplicity increase. A decrease of the parameters
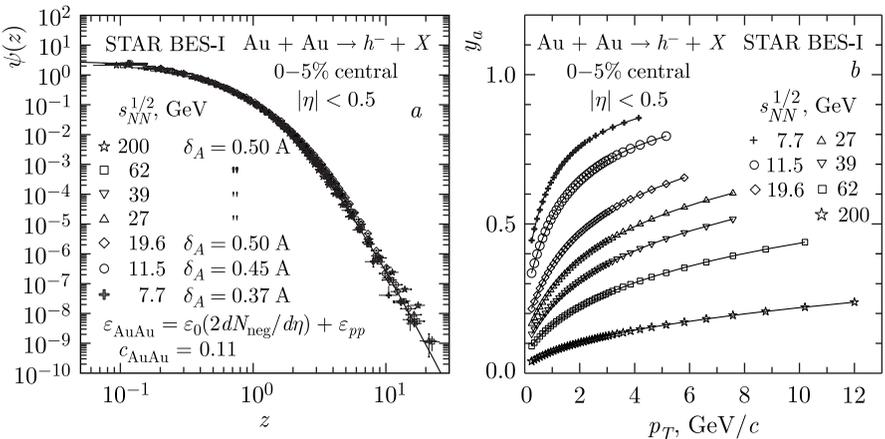

Fig. 5. Scaling function $\psi(z)$ (a) and the momentum fraction y_a in dependence on the transverse momentum p_T (b) for negative hadrons produced in $0-5\%$ central Au + Au collisions at $\sqrt{s_{NN}} = 7.7$, 11.5, 19.6, 27, 39, 62.4, and 200 GeV [21]. The symbols correspond to experimental data [82] measured by the STAR collaboration at RHIC

δ_{Au}, δ, and ε_{pp} with energy for $\sqrt{s_{NN}} < 19.6$ GeV indicates smearing of the manifestations of fractality of the interacting objects and fragmentation process at low energies.

The z-scaling of negative hadron production in $\mathrm{Au} + \mathrm{Au}$ collisions was found in the environment with different multiplicity densities. The multiplicity scan of particle yields in nucleus–nucleus collisions at different energies gives complementary information on the production mechanisms in nuclear medium. The scaling can be interpreted as a result of a self-similar modification of elementary subprocesses by the created medium. We assume that verification of the scaling behavior of $\psi(z)$ at even higher (lower) z at high multiplicities could give new restrictions on the model parameters. Based on the self-similarity arguments, one can search for changes of the scaling parameters in the nuclear systems relative to ones established in $p + p$ interactions. A discontinuity or abrupt change of the structural (δ_A) and fragmentation (ε_{AA}) fractal dimensions and the "specific heat" (c_{AA}) may indicate a signature of a phase transition or a critical point in the matter produced in nuclei collisions. Therefore, quest for irregularities in the behavior of the z-scaling parameters is inspired by searching of the location of a phase boundary and a critical point, which is of great interest.

The increase of $\varepsilon_{\mathrm{AuAu}}$ with multiplicity density is connected with a decrease of the momentum fraction y_a, representing larger energy loss in final state for large centralities (multiplicities). The value of y_a is a characteristic which describes relative energy dissipation $\Delta E_q / E_q = (1 - y_a)$ in the final state by production of an inclusive particle. The energy losses depend on the traversed medium which converts them into the multiplicity of the produced particles. This leads to the fact that the more produced multiplicity $N_{\mathrm{ch}}^{AA} \simeq$ $\simeq 2 N_{\mathrm{neg}}^{AA}$ per unit of (pseudo)rapidity, the larger energy loss of the secondary particles. The multiplicity density characterizes the produced medium and is connected in this way to the energy loss in this medium.

The amount of the relative energy loss, expressed by y_a and its dependence on $\sqrt{s_{NN}}$, multiplicity, and transverse momentum of produced particle, has relevance to the evolution of the matter created in nuclei collisions. The energy and multiplicity characteristics of the energy loss can be sensitive to the nature of the medium and can reflect changes in the fragmentation process which may occur by production of inclusive particles. Figure 5, b shows the dependence of the fraction y_a on the transverse momentum p_T for h^- hadrons produced in the $0-5\%$ central $\mathrm{Au} + \mathrm{Au}$ collisions for different energies. A monotonic growth of y_a with the momentum p_T is found for all energies. This means that the relative energy dissipation associated with the production of a high-p_T particle is smaller than for the inclusive process with lower transverse momenta. At given p_T, the decrease of y_a with $\sqrt{s_{NN}}$ shows considerable growth of the relative energy loss as the collision energy increases.

11

3. z-SCALING AND ENTROPY

The parameters used in the z-scaling scheme can be interpreted in terms of some thermodynamic quantities (entropy, specific heat, chemical potential) of a multiple particle system. There exists a profound connection between the variable z and entropy [18, 19]. The scaling variable is proportional to the ratio

$$z \sim \frac{\sqrt{s_\perp}}{W} \tag{7}$$

of the transverse kinetic energy $\sqrt{s_\perp}$ and the maximal value of the function

$$W(x_1, x_2, y_a, y_b) = \left(\frac{dN_{\text{ch}}}{d\eta} \bigg|_0 \right)^c \Omega(x_1, x_2, y_a, y_b) \tag{8}$$

in the space of the momentum fractions, constrained by condition (3). The function W is proportional to the number of all parton and hadron configurations of the colliding system which contain the constituent configuration defined by particular values of the momentum fractions x_1, x_2, y_a, and y_b.

According to statistical physics, entropy of a system is given by a number W_S of its statistical states as follows:

$$S = \ln W_S. \tag{9}$$

The most likely configuration of the system is given by the maximal value of S. For the inclusive reactions, the quantity W_S is the number of all parton and hadron configurations in the initial and final states of the colliding system which can contribute to the production of inclusive particle. The configurations comprise all constituent configurations that are mutually connected by independent subprocesses. The binary subprocesses corresponding to the production of the inclusive particle with the 4-momentum p are subject to condition (3). The underlying subprocess, which defines the variable z, is singled out from these subprocesses by the principle of maximal entropy S. The absolute number of the configurations, $W_S = W \cdot W_0$, is given up to a multiplicative constant W_0. Its value is restricted by the positiveness of entropy above some scale characterized by a maximal resolution $(\Omega^{-1})_{\text{max}}$. For the infinite resolution at fractal limit, W_0 is classically infinite. Denoting $S_0 = \ln W_0$ and using relations (2), (8), and (9), we write the entropy of system of the considered configurations as follows:

$$S = c \ln \left(\frac{dN_{\text{ch}}}{d\eta} \bigg|_0 \right) + \ln(1 - x_1)^{\delta_1} (1 - x_2)^{\delta_2} (1 - y_a)^{\varepsilon_a} (1 - y_b)^{\varepsilon_b} + S_0. \tag{10}$$

In thermodynamics, the entropy for an ideal gas is given by the formula

$$S = c_V \ln T + R \ln V + S_0. \tag{11}$$

12

Here R is a universal constant. The specific heat c_V, temperature T, and volume V characterize a state of the system.

There is an analogy between expressions (10) and (11). The analogy is supported by the plausible idea that interactions of the extended objects like hadrons and nuclei can be treated at sufficiently high energies as a set of independent collisions of their constituents. Such a concept justifies a division of the system into the part comprising a binary subprocess which can contribute to production of the inclusive particle with 4-momentum p, and the remaining part containing all other microscopic configurations which lead to the produced multiplicity. Maximization of entropy (10), constrained by condition (3), corresponds to the maximal entropy of the remaining part of the system. The multiplicity density of particles produced in the central interaction region characterizes a "temperature" created in the system. Provided the system is in a local equilibrium, there exists a simple relation $dN_{\mathrm{ch}}/d\eta|_0 \sim T^3$ for high temperatures and small chemical potentials. Using the mentioned analogy, the model parameter c plays a role of a "specific heat" of the produced matter. The second term in (10) depends on the volume of the rest of the system in the space of the momentum fractions $\{x_1, x_2, y_a, y_b\}$. The volume is a product of the complements of the fractions with exponents which are generally fractional numbers, $V = l_1^{\delta_1} l_2^{\delta_2} l_a^{\varepsilon_a} l_b^{\varepsilon_b}$. This analogy emphasizes once more the interpretation of the model parameters $\delta_1, \delta_2, \varepsilon_a$, and ε_b as fractal dimensions.

Entropy (10) increases with the multiplicity density $dN_{\mathrm{ch}}/d\eta|_0$ and decreases with the increasing resolution Ω^{-1}. The minimal resolution with respect to all binary subprocesses satisfying condition (3), which singles out the corresponding subprocess, is equivalent to the maximal entropy S of the rest of the system.

3.1. Maximum Entropy Principle and Conservation of Fractal Cumulativity. According to the assumption of fractal self-similarity of hadron structure and fragmentation process and due to the locality of binary interactions of hadron constituents, there exists a conservation law of a scale-dependent quantity characterizing hadron interactions at a constituent level. The quantification of such a statement is based on the maximum entropy principle. The conservation law reflects a symmetry of transformation of one fractal structure into another one at all scales. The corresponding symmetry is encoded in the functional form of the fractions x_1, x_2, y_a, y_b which follows from the requirement of maximal entropy (10). The conditions for the maximization of the entropy with constraint (3) determine specific dependences of the fractions on the kinematics of the inclusive reaction. As shown in [83], the momentum fractions satisfy the following equality:

$$\delta_1 \frac{x_1}{1 - x_1} + \delta_2 \frac{x_2}{1 - x_2} = \varepsilon_a \frac{y_a}{1 - y_a} + \varepsilon_b \frac{y_b}{1 - y_b}. \tag{12}$$

This equation represents a conservation law for the quantity

$$C(D, \zeta) = Dg(\zeta), \quad g(\zeta) = \frac{\zeta}{1 - \zeta}. \tag{13}$$

The symbol D means a fractal dimension and ζ is the corresponding momentum fraction. Conservation law (12) holds for any inclusive reaction with arbitrary momenta P_1, P_2, and p of the colliding and inclusive particles which determine corresponding level of resolution. We name the quantity $C(D, \zeta)$ as the "fractal cumulativity" of a fractal-like structure with the dimension D carried by its constituent with the momentum fraction ζ. The conservation law for this quantity is formulated as follows:

The fractal cumulativity before a constituent interaction is equal to that after the constituent interaction for any binary constituent subprocess,

$$\sum_i^{\text{in}} C(D_i, \zeta_i) = \sum_j^{\text{out}} C(D_j, \zeta_j). \tag{14}$$

The quantity $C(D, \zeta)$ characterizes the property of a fractal-like object or a fractal-like process with the dimension D to form a structural aggregate with certain degree of local compactness, which carries its momentum fraction ζ. The value of the fractal cumulativity is a measure of the ability of the fractal systems to create the aggregated substructures. This cumulative feature of the internal structure of hadrons and nuclei is connected with formation of hadron constituents interacting in the underlying subprocesses locally. It is in agreement with the Heisenberg uncertainty principle. The aggregation property in the final state concerns formation of the produced particles in the fractal-like fragmentation process.

The scale dependence of the conserved quantity $C(D, \zeta)$ is given by the function $g(\zeta)$. Due to the general way of its derivation, the form of $g(\zeta)$ is the same for arbitrary fractal objects (different hadrons, nuclei, hadron constituents, jets, guarks, gluons, etc.) participating in the high energy interactions. The dimension D is considered to be a new and unique characteristic of the related fractal structures, such as mass, charge, and spin. The fractal cumulativity corresponding to different momentum fractions satisfies the following relations:

$$C(D, \zeta'') = C(D, \zeta) + C(D, \zeta') + D^{-1}C(D, \zeta)C(D, \zeta'), \tag{15}$$
$$\zeta'' = \zeta + \zeta' - \zeta\zeta'. \tag{16}$$

This is a composition rule connecting the values of the cumulativity $C(D, \zeta)$ of the same fractal structure at different levels of its aggregation.

We would like to note that (12) was derived by the formulae expressed in terms of the Lorentz invariant quantities. It means that the conservation law for the fractal cumulativity holds in any motion inertial frame in the unchanged form. The cumulativity $C(D, \zeta)$ is therefore a relativistic invariant with respect to motion. The quantity manifests itself in hadron interactions at

a constituent level. Large values of the fractal cumulativity of the interacting hadron structures can be obtained by increasing the resolution or compactness of the system. The state of resolution revealed in measurements of the inclusive particles depends on fractal dimensions of the interacting objects and fractal dimensions of the fragmentation processes in the final state.

3.2. Entropy Decomposition and Quantization of Fractal Dimensions. The fractality of hadron structure and fragmentation process manifests itself most prominently near the kinematic limit $(x_1, x_2, y_a, y_b) \to 1$ of the inclusive reaction. The entropy of the constituent configurations in this region bears information on fractal characteristics of hadron interactions at small scales. In the vicinity of the kinematic limit (i.e., near the fractal limit $\Omega^{-1} \to \infty$), the momentum-dependent part

$$S_\Omega = \delta_1 \ln (1-x_1) + \delta_2 \ln (1-x_2) + \varepsilon_a \ln (1-y_a) + \varepsilon_b \ln (1-y_b) + \ln \Omega_0 \quad (17)$$

of entropy (10) can be expressed in the form that admits physical interpretation of quantization of the fractal dimensions δ_1, δ_2, ε_a, and ε_b.

The maximization of S_Ω constrained by condition (3) gives the asymptotic formulae [83]

$$1 - x_1 = h_1(p)\frac{\delta_1}{\delta + \varepsilon}, \qquad 1 - x_2 = h_2(p)\frac{\delta_2}{\delta + \varepsilon}, \qquad (18)$$

$$1 - y_a = h_a(p)\frac{\varepsilon_a}{\delta + \varepsilon}, \qquad 1 - y_b = h_b(p)\frac{\varepsilon_b}{\delta + \varepsilon}, \qquad (19)$$

valid near the kinematic boundary. The functions $h_1(p)$, $h_2(p)$, $h_a(p)$, $h_b(p)$ depend explicitly on the momentum p of the inclusive particle, $\delta \equiv \delta_1 + \delta_2$ and $\varepsilon \equiv \varepsilon_a + \varepsilon_b$. Using expressions (18) and (19), entropy (17) can be decomposed as follows:

$$S_\Omega = S_\Upsilon - S_\Gamma + \ln \Omega_0. \qquad (20)$$

The first term, S_Υ, describes the dependence of the entropy on the momenta and masses of the colliding and inclusive particles, the second term,

$$S_\Gamma = (\delta + \varepsilon) \ln(\delta + \varepsilon) - \delta_1 \ln \delta_1 - \delta_2 \ln \delta_2 - \varepsilon_a \ln \varepsilon_a - \varepsilon_b \ln \varepsilon_b, \qquad (21)$$

depends solely on fractal dimensions, and the third one is a constant that guarantees normalization. Formula (21) allows us to derive physical consequences provided that the fractal dimensions are expressed as integer multiples of the same constant d,

$$\delta_1 = n_{\delta_1}d, \quad \delta_2 = n_{\delta_2}d, \quad \varepsilon_a = n_{\varepsilon_a}d, \quad \varepsilon_b = n_{\varepsilon_b}d. \qquad (22)$$

In that case, the entropy S_Γ can be interpreted within a statistical ensemble of fractal configurations of the internal structures of the colliding hadrons (or nuclei) and fractal configurations corresponding to the fragmentation processes in the final state. The statistical ensemble is considered as a collection of n_{δ_1} fractals with random configurations but with the same fractal dimension δ_1, together with an analogous set of n_{δ_2} interacting fractals with the fractal dimension δ_2, which are combined via binary subprocesses with the

collection of n_{ε_a} fractals with random configurations but with the same fractal dimension ε_a in the final state, and the corresponding set of n_{ε_b} fractals with the fractal dimension ε_b. For large numbers of the configurations, S_Γ can be rewritten as follows:

$$S_\Gamma = d \ln\left(\Gamma_{\delta_1,\delta_2,\varepsilon_a,\varepsilon_b}\right), \tag{23}$$

where

$$\Gamma_{\delta_1,\delta_2,\varepsilon_a,\varepsilon_b} \equiv \frac{(n_{\delta_1} + n_{\delta_2} + n_{\varepsilon_a} + n_{\varepsilon_b})!}{n_{\delta_1}!\, n_{\delta_2}!\, n_{\varepsilon_a}!\, n_{\varepsilon_b}!} = \Gamma_{\delta,\varepsilon}\Gamma_{\delta_1,\delta_2}\Gamma_{\varepsilon_a,\varepsilon_b} \tag{24}$$

and

$$\Gamma_{\delta,\varepsilon} = \frac{(n_\delta + n_\varepsilon)!}{n_\varepsilon!\, n_\delta!}, \quad \Gamma_{\delta_1,\delta_2} = \frac{(n_{\delta_1} + n_{\delta_2})!}{n_{\delta_1}!\, n_{\delta_2}!}, \quad \Gamma_{\varepsilon_a,\varepsilon_b} = \frac{(n_{\varepsilon_a} + n_{\varepsilon_b})!}{n_{\varepsilon_a}!\, n_{\varepsilon_b}!}. \tag{25}$$

According to statistical physics, formulae (23)–(25) give us the possibility to interpret the entropy S_Γ, expressed in units of the dimensional quantum d, as the logarithm of the number of different ways, $\Gamma_{\delta_1,\delta_2,\varepsilon_a,\varepsilon_b}$, in which the fractal dimensions of the interacting fractal structures can be composed of the identical dimensional quanta, each of the size d. The symbol $\Gamma_{\delta,\varepsilon}$ represents the number of ways how the overall number $n = n_\delta + n_\varepsilon$ of the dimensional quanta can be shared among n_δ portions pertaining to the fractal dimensions of the colliding objects and n_ε portions belonging to the fractal dimensions characterizing fractal structures of the fragmentation processes. The symbols $\Gamma_{\delta_1,\delta_2}$ and $\Gamma_{\varepsilon_a,\varepsilon_b}$ represent the numbers of ways in which the corresponding numbers $n_\delta = n_{\delta_1} + n_{\delta_2}$ and $n_\varepsilon = n_{\varepsilon_a} + n_{\varepsilon_b}$ of the dimensional quanta can be distributed between the fractal dimensions of the single fractals in the initial and final states, respectively.

The statistical interpretation of entropy (21) is only possible under the quantization of fractal dimensions (22), where d is an elementary dimensional quantum. The quantization is a kind of ordering that diminishes the total entropy (S_Γ enters with minus sign into Eq. (20)).

3.3. Conservation of the Number of Cumulativity Quanta. The quantization of the fractal dimension, $D = n_D d$, is connected with quantum character of the fractal cumulativity $C(D,\zeta)$. Using expression (13), we can write this quantity in the form

$$C = n_C d, \qquad n_C(n_D, \zeta) = n_D \frac{\zeta}{1 - \zeta}, \tag{26}$$

where $n_C(n_D, \zeta)$ represents the number of quanta of the fractal cumulativity expressed in units of the dimensional quantum d. The quantum character of the fractal dimensions has profound impact on the physical content of the conservation law for the fractal cumulativity. According to (12), the number of the cumulativity quanta is conserved at any resolution given by arbitrary momenta P_1, P_2, and p of the colliding and inclusive particles. The conservation law can be formulated as follows:

The number of quanta of fractal cumulativity before a constituent interaction is equal to that after the constituent interaction for any binary subprocess,

$$\sum_i^{\text{in}} n_C(n_{D_i}, \zeta_i) = \sum_j^{\text{out}} n_C(n_{D_j}, \zeta_j). \tag{27}$$

The quantization of the dimension D and cumulativity $C(D, \zeta)$ is based on the assumptions of the fractal self-similarity of internal hadron structure, fractal nature of fragmentation process, and locality of hadron interactions at a constituent level up to the kinematic limit.

The conservation law for the quanta of the fractal cumulativity follows from general physical principles. According to the Noether's theorem, for every conservation law of a continuous quantity there must be a continuous symmetry. In our case, the corresponding symmetry is a scale-dependent translation symmetry which guarantees the conservation law for the fractal cumulativity at any scale fixed by the minimal necessary level of resolution.

CONCLUSIONS

In summary, we conclude that z-scaling is a specific feature of high-p_T particle production established in $p + p$ and $\overline{p} + p$ collisions at U70, ISR, Sp$\overline{p}$S, Tevatron, RHIC, and LHC. It reflects the self-similarity, locality, and fractality of hadron interactions at a constituent level. The scaling behavior was confirmed for inclusive production of different hadrons, jets, heavy quarkonia, and top quark. The hypothesis of the self-similarity and fractality was tested in $Au + Au$ collisions at RHIC using z-presentation of spectra of negative hadrons. The analysis of the STAR BES-I data indicates energy and multiplicity independence of the scaling function $\psi(z)$. The variable z depends on the multiplicity density, "heat capacity", and entropy of constituent configurations of the interacting system. The constituent energy loss as a function of the energy and centrality of collisions and the transverse momentum of inclusive particles was estimated.

We have shown that z-scaling, containing the principle of maximum entropy, includes a conservation law of the "fractal cumulativity" $C(D, \zeta)$. This quantity reflects the ability of the fractal systems to create structural constituents with certain degree of local compactness. The cumulativity of a fractal object or a fractal-like process with fractal dimension D carried by its constituent with the momentum fraction ζ is proportional to the dimension D and represents a simple function of ζ. It was shown that a composition rule for $C(D, \zeta)$ connects the fractal cumulativity at different scales. The fractal dimension D is interpreted as a quantity which has quantum nature. The quantization of fractal dimensions results in preservation of the number of the cumulativity quanta $n_C(n_D, \zeta)$ in binary subprocesses at any resolution.

REFERENCES

1. *Eichten E., Lane K., Peskin M.* // Phys. Rev. Lett. 1983. V. 50. P. 811.
2. *Eichten E., Hinchliffe I., Lane K., Quigg C.* // Rev. Mod. Phys. 1984. V. 56. P. 4.
3. *Antoniadis I.* // Phys. Lett. B. 1990. V. 246. P. 377.
4. *Arkani-Hamed N., Dimopoulos S., Dvali G. R.* // Phys. Lett. B. 1998. V. 429. P. 263.
5. *Antoniadis I., Arkani-Hamed N., Dimopoulos S., Dvali G. R.* // Phys. Lett. B. 1998. V. 436. P. 257.
6. *Randall L., Sundrum R.* // Phys. Rev. Lett. 1999. V. 83. P. 3370.
7. *Randall L., Sundrum R.* // Phys. Rev. Lett. 1999. V. 83. P. 4690.
8. *Dimopoulos S., Landsberg G. L.* // Phys. Rev. Lett. 2001. V. 87. P. 161602.
9. *Giddings S. B., Thomas S. D.* // Phys. Rev. D. 2002. V. 65. P. 056010.
10. *Barrau A., Grain J., Alexeyev S.* // Phys. Lett. B. 2004. V. 584. P. 114.
11. *Mandelbrot B.* The Fractal Geometry of Nature. San Francisco: Freeman, 1982.
12. *Nottale L.* Fractal Space-Time and Microphysics. Singapore: World Sci., 1993.
13. *Feder J.* Fractals. New York: Plenum Press, 1988.
14. *Lederman L. M., Hill C. T.* Symmetry and the Beautiful Universe. Amherst, NY: Prometheus Books, 2004.
15. *Stanley H. E.* Introduction to Phase Transitions and Critical Phenomena. Oxford: Oxford Univ. Press, 1971.
16. *Stanley H. E.* // Rev. Mod. Phys. 1999. V. 71. P. S358.
17. *Domb C.* The Critical Point: A Historical Introduction to the Modern Theory of Critical Phenomena. London: Taylor and Francis, 1996.
18. *Zborovský I., Tokarev M. V.* // Phys. Rev. D. 2007. V. 75. P. 094008.
19. *Zborovský I., Tokarev M. V.* // Intern. J. Mod. Phys. A. 2009. V. 24. P. 1417.
20. *Tokarev M. V., Zborovský I.* // Intern. J. Mod. Phys. A. 2017. V. 32. P. 1750029.
21. *Tokarev M., Kechechyan A., Zborovský I.* // Nucl. Phys. A. 2020. V. 993. P. 121646.
22. *Tokarev M. V., Zborovský I., Kechechyan A. O., Dedovich T. G.* // Phys. Part. Nucl. 2020. V. 51. P. 141.
23. *Albrow M. G. et al. (CHLM Collab.)* // Nucl. Phys. B. 1973. V. 56. P. 333.
24. *Alper B. et al. (BS Collab.)* // Nucl. Phys. B. 1975. V. 100. P. 237.
25. *Büsser F. W. et al. (CCRS Collab.)* // Nucl. Phys. B. 1976. V. 106. P. 1.
26. *Guettler K. et al. (BSM Collab.)* // Phys. Lett. B. 1976. V. 64. P. 111.
27. *Guettler K. et al. (BSM Collab.)* // Nucl. Phys. B. 1976. V. 116. P. 77.
28. *Antreasyan D. et al.* // Phys. Rev. D. 1979. V. 19. P. 764.
29. *Drijard D. et al. (CDHW Collab.)* // Nucl. Phys. B. 1982. V. 208. P. 1.
30. *Jaffe D. E. et al.* // Phys. Rev. D. 1989. V. 40. P. 2777.
31. *Adams J. et al. (STAR Collab.)* // Phys. Lett. B. 2005. V. 616. P. 8.
32. *Adams J. et al. (STAR Collab.)* // Phys. Lett. B. 2006. V. 637. P. 161.
33. *Abelev B. I. et al. (STAR Collab.)* // Phys. Rev. C. 2007. V. 75. P. 064901.
34. *Adams J. et al. (STAR Collab.)* // Phys. Rev. C. 2005. V. 71. P. 064902.
35. *Abelev B. I. et al. (STAR Collab.)* // Phys. Rev. Lett. 2006. V. 97. P. 132301.
36. *Witt R. (for the STAR Collab.)* // J. Phys. G: Nucl. Part. Phys. 2005. V. 31. P. S863.
37. *Adare A. et al. (PHENIX Collab.)* // Phys. Rev. D. 2011. V. 83. P. 052004.
38. *Agakishiev G. et al. (STAR Collab.)* // Phys. Rev. Lett. 2012. V. 108. P. 072302.

39. *Adare A. et al. (PHENIX Collab.)* // Phys. Rev. C. 2014. V. 90. P. 054905.
40. *Adams J. et al. (STAR Collab.)* // Phys. Rev. Lett. 2004. V. 92. P. 112301.
41. *Büsser F. W. et al. (CCRS Collab.)* // Phys. Lett. B. 1976. V. 61. P. 309.
42. *Kichimi H. et al.* // Phys. Rev. D. 1979. V. 20. P. 37.
43. *Drijard D. et al. (CDHW Collab.)* // Z. Phys. C. 1982. V. 12. P. 217.
44. *Akesson T. et al. (AFS Collab.)* // Nucl. Phys. B. 1982. V. 203. P. 27; Erratum // Nucl. Phys. B. 1983. V. 229. P. 541.
45. *Adams J. et al. (STAR Collab.)* // Phys. Lett. B. 2005. V. 612. P. 181.
46. *Aduszkiewicz A. et al. (NA61/SHINE Collab.)* // Eur. Phys. J. C. 2016. V. 76. P. 198.
47. *Afanasiev S. V. et al. (NA49 Collab.)* // Phys. Lett. B. 2000. V. 491. P. 59.
48. *Anticic T. et al. (NA49 Collab.)* // Phys. Rev. C. 2011. V. 84. P. 064909.
49. *Abe F. et al. (CDF Collab.)* // Phys. Rev. Lett. 1995. V. 74. P. 2626.
50. *Abachi S. et al. (DØ Collab.)* // Phys. Rev. Lett. 1995. V. 74. P. 2632.
51. *Abazov V. M. et al. (DØ Collab.)* // Phys. Lett. B. 2010. V. 693. P. 515.
52. *Chatrchyan S. et al. (CMS Collab.)* // Eur. Phys. J. C. 2013. V. 73. P. 2339.
53. *Khachatryan V. et al. (CMS Collab.)* // Eur. Phys. J. C. 2015. V. 75. P. 542.
54. *Khachatryan V. et al. (CMS Collab.)* // Phys. Rev. D. 2016. V. 94. P. 072002.
55. *CMS Collab.* CMS PAS TOP-16-011.
56. *Aad G. et al. (ATLAS Collab.)* // Phys. Rev. D. 2014. V. 90. P. 072004.
57. *Aad G. et al. (ATLAS Collab.)* // JHEP. 2015. V. 06. P. 100.
58. *Aad G. et al. (ATLAS Collab.)* // Phys. Rev. D. 2016. V. 93. P. 032009.
59. *Aad G. et al. (ATLAS Collab.)* // Eur. Phys. J. C. 2016. V. 76. P. 538.
60. *Abazov V. M. et al. (DØ Collab.)* // Phys. Rev. D. 2014. V. 90. P. 092006.
61. *Aad G. et al. (ATLAS Collab.)* // Eur. Phys. J. C. 2013. V. 73. P. 2509.
62. *Aad G. et al. (ATLAS Collab.)* // Phys. Rev. D. 2012. V. 86. P. 014022.
63. *Aaboud M. et al. (ATLAS Collab.)* // JHEP. 2017. V. 09. P. 020.
64. *CMS Collab.* PAS-SMP-12-012.
65. *Chatrchyan S. et al. (CMS Collab.)* // Phys. Rev. D. 2013. V. 87. P. 112002.
66. *Abelev B. et al. (ALICE Collab.)* // Phys. Lett. B. 2013. V. 722. P. 262.
67. *Abbott B. et al. (DØ Collab.)* // Phys. Rev. D. 2001. V. 64. P. 032003.
68. *Elvira V. D.* Measurement of the Inclusive Jet Cross Sections at $\sqrt{s} = 1.8$ TeV with the DØ Detector. Ph.D Thesis. Universidad de Buenos Aires, Argentina, 1995.
69. *Abazov V. M. et al. (DØ Collab.)* // Phys. Lett. B. 2002. V. 525. P. 211.
70. *Abazov V. M. et al. (DØ Collab.)* // Phys. Rev. Lett. 2008. V. 101. P. 062001.
71. *Begel M. (for the DØ Collab.).* hep-ex/0305072.
72. *Abazov V. M. et al. (DØ Collab.)* // Phys. Rev. D. 2012. V. 85. P. 052006.
73. *Abe F. et al. (CDF Collab.)* // Phys. Rev. Lett. 1996. V. 77. P. 438.
74. *Affolder T. et al. (CDF Collab.)* // Phys. Rev. D. 2001. V. 64. P. 032001; Erratum // Phys. Rev. D. 2002. V. 65. P. 039903.
75. *Abulencia A. et al. (CDF Collab.)* // Phys. Rev. Lett. 2006. V. 96. P. 122001.
76. *Abulencia A. et al. (CDF Collab.)* // Phys. Rev. D. 2006. V. 74. P. 071103(R).
77. *Abulencia A. et al. (CDF Collab.)* // Phys. Rev. D. 2007. V. 75. P. 092006.
78. *Aaltonen T. et al. (CDF Collab.)* // Phys. Rev. D. 2008. V. 78. P. 052006; Erratum // Phys. Rev. D. 2009. V. 79. P. 119902.
79. *Tokarev M. V., Zborovský I., Dedovich T. G.* // Intern. J. Mod. Phys. A. 2012. V. 27. P. 1250115.

80. *Aggarwal M. M. et al. (STAR Collab.).* An Experimental Exploration of the QCD Phase Diagram: The Search for the Critical Point and the Onset of Deconfinement. arXiv:1007.2613.
81. *Abelev B. I. et al. (STAR Collab.)* // Phys. Rev. C. 2017. V. 96. P. 044904.
82. *Tokarev M. (for the STAR Collab.)* // Intern. J. Mod. Phys. Conf. Ser. 2015. V. 39. P. 1560103.
83. *Zborovský I.* // Intern. J. Mod. Phys. A. 2018. V. 33. P. 1850057.